Int. J. Heat Mass Transfer. Vol. 20, pp. 711–723. Pergamon Press 1977. Printed in Great Britain

A PREDICTION OF THE BOUNDS ON THE EFFECTIVE THERMAL CONDUCTIVITY OF GRANULAR MATERIALS

R. A. CRANE* and R. I. VACHON†

(*Received* 17 *December* 1974 *and in revised form* 20 *October* 1975)

Abstract—Two models are developed to describe the effective thermal conductivity of randomly packed granular systems based on a one dimensional Ohm's Law method. These models are shown to represent upper and lower bounds on the effective conductivity of all normally distributed stochastic mixtures. An empirical factor has been obtained to account for three dimensional thermal effects. Comparisons to experimental data indicate that the modified correlation is generally accurate to within $\pm 20\%$ over a wide range of constituent materials.

NOMENCLATURE

- A, area of heat transfer;
- k_c, thermal conductivity of continuous phase;
- k_d, thermal conductivity of discontinuous phase;
- k_{e_0}, effective thermal conductivity assuming uniform heat flux;
- k_{e_∞}, effective thermal conductivity assuming parallel isotherms;
- R, thermal resistance;
- t, time;
- $\bar{\varepsilon}$, solid fraction of granular material;
- μ, mode of solid fraction distribution;
- σ, standard deviation of solid fraction distribution.

1. INTRODUCTION

THE PROBLEM of determining the effective thermal conductivity of randomly packed granular materials is one which frequently occurs in engineering practice. As a consequence there has been a considerable effort in the past to develop suitable analytical models. In general these models have proved satisfactory provided that the constituent conductivities are of similar magnitude. For heterogeneous systems which do not fulfil this condition it has been found that available analytical models produce considerable error [1].

The difficulty in developing an adequate model does not arise from any ignorance of the fundamental laws, rather the problem arises in complications in their application. A detailed solution of the conduction problem would require a knowledge of the shape, size, location and conductivity of each particle in the system together with the interaction between particles. Such knowledge is difficult to represent for randomly packed systems. To overcome these difficulties, investigators have tended to make a series of simplifying assumptions. The two basic approaches may generally be classified as follows:

1. Fourier's Law models—These models utilize an idealized geometry for which the temperature field may be solved. Knowing the temperature field the effective thermal conductivity may be solved using the Fourier–Biot Law. The idealized geometry will differ significantly from the geometry of randomly packed structures. The formulations so developed are extrapolated to randomly packed systems and differ primarily in the extrapolation technique.

2. Ohm's Law models—Simplified repetitive geometries are assumed to be representative of the randomly packed system. The problem is further simplified by assuming one dimensional heat transfer. An equivalent electrical network is then developed and the thermal conductivity of the system is obtained from the thermal-electrical analogy.

2. OHM'S LAW MODELS

The Fourier's Law models received considerable attention during the early period of model development for heterogeneous systems. More recently attention has centered more toward the Ohm's Law models. Actually there exist only a very limited number of configurations for which closed form solutions exist for the Fourier equation. Once these solutions were exhausted researchers were forced toward development of the Ohm's Law models in hopes of developing a more general solution.

A simple Ohm's Law model is shown in Fig. 1(a). Here a heterogeneous material with solid volume fraction $\bar{\varepsilon}$, is represented as a series of idealized cubic particles arranged in a square array. The uniform spacing between particles is maintained such that the idealized system retains the proper volume fractions. A typical unit cell is shown in the figure. It is assumed that the effective thermal conductivity may be determined by considering the equivalent electrical resistances in parallel and in series and by applying Ohm's Law. In taking such an approach it is necessary to assume one dimensional heat transfer. Two options occur here: It may be assumed that the heat flux is uniform in the direction of heat transfer or that the isotherms are straight and parallel. These two assumptions lead respectively to the equivalent electrical networks shown in Figs. 1(b) and (c).

It should be noted that the two networks result in dif-

*Assistant Professor, Mechanical Engineering Department, University of South Florida.

†Professor, Mechanical Engineering Department, Auburn University, Auburn, AL 36830, U.S.A.

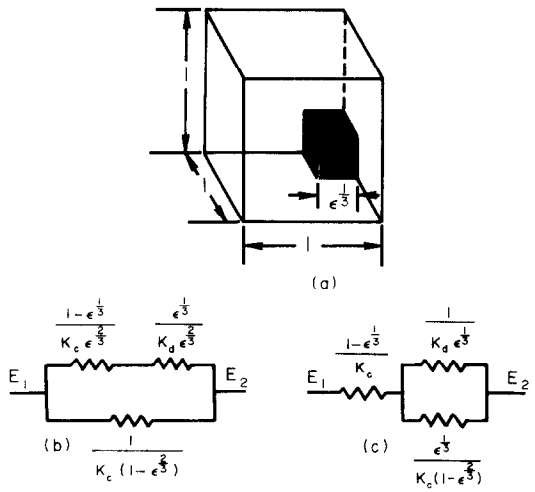

FIG. 1. Cubic lattice representation of granular material.

ferent effective conductivities. Both are approximations to the exact solution and differ because of the simplifying assumptions. It is important to note that both solutions form bounds to the real solution to the proposed model. This is more clearly seen when one considers a nodal point representation of the temperature field in the proposed system. If the resistances normal to the direction of heat flow are assumed to be very large, the heat flow will remain uniform in the direction of the overall temperature gradient. Conversely, if the lateral resistances are taken as zero the potential will be equal in each lateral plane. Therefore, the assumption of linear and parallel heat flux lines is equivalent to the assumption of infinite lateral resistances; the assumption of parallel isotherms is equivalent to that of zero lateral resistance. The actual resistance will, of course, fall somewhere between zero and infinity so that these two cases form the bounding conditions. Whether the two solutions represent the bounding conditions for the physical system depends upon the suitability of the proposed model. It can therefore be stated that the limitations placed on available Ohm's Law models may be attributed to two principle causes:

1. Unrealistic Geometrical Assumptions—Most common Ohm's Law models utilize highly idealized particle shapes (usually parallelopipeds) and unrealistic particle arrays (usually cubic). Both assumptions deviate significantly from the physical situation found in randomly packed granular materials frequently found in nature.
2. Unrealistic Heat Flow Assumptions—The assumption of one dimensional heat flow, which is almost universally to be found in Ohm's Law models, is not justified for systems with constituents of widely differing thermal conductivities.

Any model development which might serve to eliminate or reduce differences between the analytical model and actual granular systems should also serve to extend the range of applicability of the proposed correlation.

3. THEORETICAL DEVELOPMENT

Recognizing the two principal causes of failure for existing correlations, it has been decided to approach them systematically, solving first the geometrical relationships. In this case fully stochastic arrangements will be used.

A. *Uniform heat flux*

Consider a typical unit cell of the heterogeneous system shown in Fig. 2(a). Divide the unit cell into uniform sized channels by passing both vertical and horizontal planes through the element. These planes are to be oriented parallel to the direction of heat flux and are to be equi-spaced. If the channels are sufficiently small compared to the dimensions of the solid particles, they will appear as consisting of sections of the continuous and discontinuous phases placed in series. Assuming a uniform heat flux in each channel, the order of the series resistances does not influence the overall resistance. Consequently, the two components may be separated as shown in Fig. 2(b). The resistance of the channel is then given by

$$R_i = \frac{\varepsilon_i}{k_d \Delta A} + \frac{(1-\varepsilon_i)}{k_c \Delta A}. \tag{1}$$

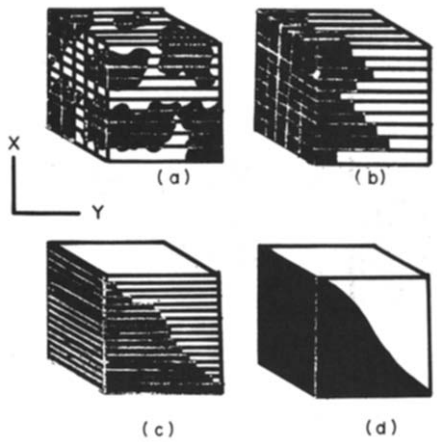

FIG. 2. Equivalent geometries for uniform heat flux.

The channels behave as resistances in parallel. The overall resistance is then given as:

$$\frac{1}{R_e} = \frac{1}{R_1} + \frac{1}{R_2} + \ldots + \frac{1}{R_n}. \tag{2}$$

The order of these channels and their shape may be altered so long as the individual channel resistances remain unchanged. They may then be distorted to a unit width by changing the vertical dimension while retaining the unit length. They are then arranged in order of decreasing solid fraction. This geometry is shown in Fig. 2(c). The effective thermal conductivity for the specified element is

$$k_{e_0} = \sum_{i=1} \frac{k_c k_d \Delta A_i}{k_c \varepsilon_i + k_d (1-\varepsilon_i)} \tag{3}$$

If the area of the channels is allowed to approach zero as the number of channels approaches infinity the

summation in equation (3) may be replaced by an integral

$$k_{e_0} = \int_A \frac{k_c k_d \, dA}{k_c \varepsilon + k_d(1-\varepsilon)} \tag{4}$$

$$k_{e_0} = \int_0^1 \int_0^1 \frac{k_c k_d}{k_d + \varepsilon(k_c - k_d)} dx \, dy \tag{5}$$

$$= \int_0^1 \frac{k_c k_d}{k_d + \varepsilon(k_c - k_d)} dx \tag{6}$$

since the integrand is constant in the horizontal direction. The corresponding geometry is shown in Fig. 2(d).

B. *Parallel isotherms*

Consider a unit cube of the heterogeneous system shown in Fig. 3(a). The system is to be divided into a series of fine lamina oriented normal to the direction of heat flow as shown. These elements are chosen to be sufficiently thin that the cross sectional area of the solid particles are essentially constant throughout its width. Assuming parallel isotherms within the unit cube, the discontinuous (solid) and continuous phases will act as resistances in parallel within each lamina.

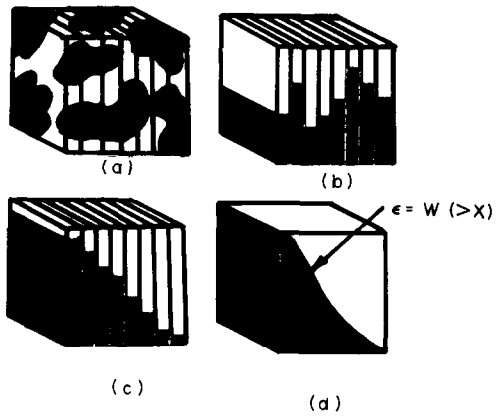

FIG. 3. Equivalent geometries for linear isotherms.

The order of the parallel resistances may be changed arbitrarily without affecting the overall resistance of the parallel circuit. Thus the resistances of the solid elements may be grouped together in each lamina as shown in Fig. 3(b). A simple calculation then shows that the equivalent resistance is given by the equation:

$$ke_\infty = \frac{1}{\sum_{m=1}^{L} \frac{\Delta x}{k_c + (k_d - k_c)\varepsilon_m}}. \tag{7}$$

Where the solid fraction in the mth lamina is given by ε_m and the width of each lamina is Δx.

Note the laminae act as resistances in series. Again the order of the resistances does not affect the overall thermal resistance so that the elements may be rearranged in order of decreasing solid fraction as shown in Fig. 3. If the width of the laminae is allowed to approach zero then the effective thermal conductivity for Fig. 3(d) becomes:

$$ke_\infty = \frac{1}{\int_0^1 \frac{dx}{k_c + (k_d - k_c)\varepsilon}}. \tag{8}$$

C. *Evaluation of the solid fraction, ε*

Both equations for zero and infinite lateral conductivity, (6) and (8), require a knowledge of the functional relation between the solid area fraction and position to solve the integral. The technique for obtaining such a relation was developed by Tsao [2]. Consider the arbitrary material distribution shown in Fig. 2(c). The vertical position of each lamina is determined by its solid fraction. The portion of the elements below a particular element is then equal to the portion of elements having larger solid fractions.

$$x = P(\varepsilon_i > \varepsilon) \tag{9}$$

$$x = \int_\varepsilon^1 f(\phi) \, d\phi. \tag{10}$$

Differentiating this equation,

$$dx = -f(\varepsilon) \, d\varepsilon. \tag{11}$$

This relationship may be substituted into equations (6) and (8) for the thermal conductivity with uniform heat flux and parallel isotherms. The limits of integration must be changed accordingly.

$$k_{e_0} = \int_1^0 \frac{k_c k_d f(\varepsilon)}{k_d + \varepsilon(k_c - k_d)} d\varepsilon \tag{12}$$

$$\frac{1}{k_{e_x}} = \int_1^0 \frac{f(\varepsilon)}{k_c + \varepsilon(k_d - k_c)} d\varepsilon. \tag{13}$$

Equations (12) and (13) are entirely general in that no assumptions have yet been made regarding the particle shape or size distribution. The effects of these parameters on the solid area fraction were studied by Debbas and Rumph [3] and Haughey and Beveridge [4]. These sources found experimentally that the distribution of the solid area fraction is Gaussian for most packings. A notable exception occurs after prolonged vibration of a sample. This packing produces large regions of ordered distribution and strong anisotropic effects. Similarly large particle size variations tend to allow sifting of smaller particles into the lower regions of a given sample. This produces a definite bulk porosity gradient in the vertical direction. In such cases the radial distribution remains normal. Neglecting all such non-normal distributions the frequency distribution may be taken as Gaussian

$$f(t) = \frac{e^{-\frac{1}{2}t^2}}{\int_a^b e^{-\frac{1}{2}t^2} dt}. \tag{14}$$

The integral in the denominator serves to normalize the truncated Gaussian distribution. By replacing the standardized random variable equation (14) may be written in the form:

$$f(\varepsilon) = \frac{+e^{-\frac{1}{2}\left(\frac{\varepsilon-\mu}{\sigma}\right)^2}}{\frac{\sigma\sqrt{\pi}}{\sqrt{2}}\left[\operatorname{erf}\left(\frac{1-\mu}{\sigma\sqrt{2}}\right) - \operatorname{erf}\left(\frac{0-\mu}{\sigma\sqrt{2}}\right)\right]}. \tag{15}$$

The mode of the distribution, μ, and the standard deviation of the solid area fraction, σ, remain to be evaluated. The mode may be defined implicitly in terms of the standard deviation from the basic geometry of

the mixture. The total solid volume is equal to the sum of the elemental solid volumes.

$$\bar{\varepsilon} = \int_0^1 \varepsilon \, dx. \tag{16}$$

Using the results of equation (11) this expression may be written:

$$\bar{\varepsilon} = \int_1^0 -\varepsilon f(\varepsilon) \, dx. \tag{17}$$

Determination of an exact expression for the standard deviation is difficult. Strange [5] reports that the standard deviation is given by the relation,

$$\sigma = \frac{\text{constant}}{\sqrt{M}} \tag{18}$$

where M is a measure of the sample size.

For the correlation to be meaningful there must exist a minimum size sample such that for all larger samples the effective thermal conductivity is constant. This is in fact the case as shown in Fig. 4. Here σ is varied in the equations for the effective thermal conductivity

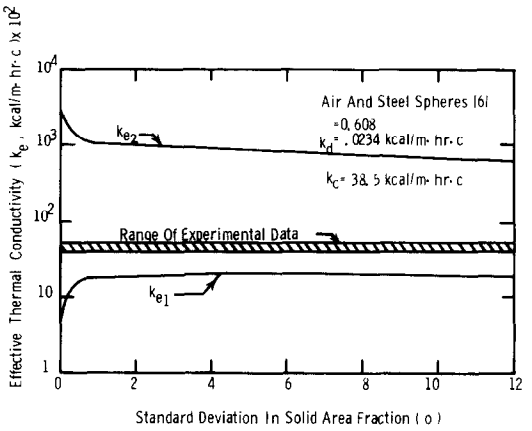

FIG. 4. Effect of standard deviation in area fraction upon effective conductivity.

using uniform heat flux and parallel isotherms respectively. It may also be noted that the calculational results bracket the range of experimental data. This is, of course, the expected trend since the assumption of uniform heat flux and parallel isotherms correspond to those of zero and infinite lateral conductivity respectively.

4. DEVELOPMENT OF AN EFFECTIVE CONDUCTIVITY CORRELATION

Equations (7) and (8) have been obtained to predict the effective thermal conductivity of two phase mixtures as a function of the constituent conductivities and the volume fractions. The distribution of the two phases is found by taking σ as any sufficiently large number, $\sigma > 100$, and solving equations (15) and (17) implicitly for the corresponding value of μ. The resulting thermal conductivity expressions are considered to be geometrically realistic for most random packings of spherical or semispherical particles but are based alternately on the assumptions of zero or infinite lateral conductivity. Since the lateral conductivity of the mixture will fall between these limits the two equations form a set of bounding limits for the physical case. Numerous authors have proposed correlations which effectively imply that one of these two assumptions is sufficiently close to the physical system that it may be used in obtaining an effective conductivity expression. In spite of arguments presented by proponents of both methods, it does not appear possible to select, *a priori*, a correlation which is more consistent with the physical system. The preferred method would then be to compare both correlations to experimental results and to make a selection based on the demonstrated results.

Such a comparison has been made and the results are shown graphically in Figs. 5–7. These figures represent randomly packed granular systems with porosities of 0.31, 0.43 and 0.58 respectively. The

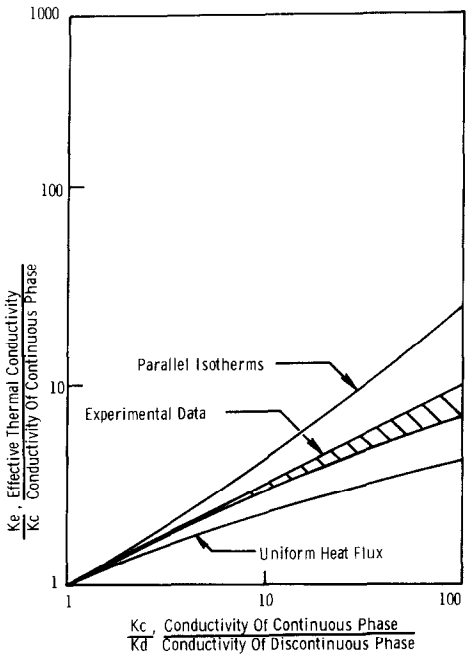

FIG. 5. Comparison of bounding conductivities with experimental data for a porosity of 0.31.

selected values represent a range of packing fractions so that they may be considered as representative of all random packings. The non-dimensionalized effective conductivity is given as a function of the constituent conductivity ratios, k_c/k_d. The experimental values are taken from data listed in Table 1. As shown in the figures virtually all data falls between the two limiting curves. For a constituent conductivity ratio, $k_d/k_c < 10$ either bounding equation gives reasonably accurate results. For $k_d/k_c > 100$ both correlations deviate significantly from the experimental data. This indicates the reason why previous Ohm's Law models have generally not been successful at higher constituent conductivity ratios. No doubt some of the discrepancy has been countered by frequently assuming a somewhat distorted array. Uniform heat flux models have been developed such that an inordinate amount of the higher conductivity material is arranged in series with itself.

Table 1. Comparison of bounding conductivities to experimental conductivities

Case	Fluid phase	Solid phase	Conductivity, (kcal/m h K) × 100 Experiment	Uniform heat flux	Parallel isotherms	(k_d/k_c)	$1-\bar{\varepsilon}$	Ref.
1	Air 2.41	Calcite 310	21.4	12.1	64.8	128.6	0.493	[6]
2	Air 2.41	Steel 1650	22.4	16.1	261.1	684.6	0.489	[7]
3	Helium 11.95	Steel 1650	75.5	60.5	341.2	138.1	0.489	[7]
4	Glycerin 45.4	Steel 1650	246.0	170.6	456.4	36.3	0.489	[7]
5	Water 51.6	Steel 1650	272.0	187.4	471.9	32.0	0.489	[7]
6	CO_2 0.080	Basalt k0.8	1.015	0.0047	2.26	134.2	0.470	[8]
7	EtOH 15.7	Calcite 310	63.6	49.9	101.0	19.7	0.465	[9]
8	Air 2.41	Calcite 310	25.0	11.9	65.7	128.6	0.458	[6]
9	Air 2.13	Calcite 310	17.5	10.6	65.7	145.5	0.454	[9]
10	EtOH 15.7	Calcite 310	63.5	48.7	10.3	19.7	0.454	[9]
11	Water 50.5	Calcite 310	127.0	103.8	154.3	6.1	0.453	[10]
12	Air 2.12	Calcite 310	19.0	10.7	64.7	146.2	0.451	[10]
13	Air 2.13	Calcite 310	17.2	10.6	65.6	145.5	0.451	[10]
14	Air 2.34	Lead 2950	30.4	16.1	455.0	1260.7	0.450	[6]
15	Water 50.8	Calcite 310	118.0	104.4	154.3	6.1	0.447	[10]
16	Air 2.38	Quartz 950	36.5	14.0	170.1	398.7	0.440	[9]
17	Air 2.34	Lead 2950	23.9	15.4	475.7	1260.7	0.439	[6]
18	Water 54.5	Silica 973.9	216.0	154.3	356.0	17.9	0.439	[7]
19	Air 2.25	Quartz 945	26.8	12.7	176.3	420.0	0.438	[11]
20	Air 2.25	Coal 36	11.8	6.2	13.6	16.0	0.437	[11]
21	Hydrogen 16.6	Coal 36	25.3	21.8	27.7	2.2	0.437	[11]
22	Air 2.308	Silica 973.9	21.89	13.0	181.7	421.9353	0.437	[7]
23	Air 2.34	Steel 3850	34.1	15.8	604.7	1645.2996	0.435	[6]
24	EtOH 29.34	Silica 973.9	144.7	98.4	302.0	33.198	0.434	[7]
25	Air 2.34	Lead 2950	34.4	15.4	475.7	1260.6841	0.433	[6]
26	Water 54.5	Silica 973.9	244.9	154.3	356.1	17.8689	0.431	[7]
27	IC8 12.29	Glass 93.96	35.14	26.5	44.6	7.6485	0.431	[7]
28	Oil 15.4	Lead 2410	81.5	73.1	533.3	156.4935	0.430	[10]
29	Water 54.5	Silica 973.9	224.9	154.3	356.1	17.8689	0.430	[7]
30	Water 54.5	Silica 973.9	217.4	154.3	356.1	17.8689	0.430	[7]
31	Water 54.5	Silica 973.9	218.9	154.3	356.1	17.8689	0.430	[7]
32	Water 54.5	Silica 973.9	218.9	154.3	356.1	17.8689	0.430	[7]
33	H_2 14.85	SiC 1550	91.0	65.0	371.3	104.3771	0.429	[12]

Table 1 *Continued*

Case	Fluid phase	Solid phase	Conductivity, (kcal/m h K) × 100 Experiment	Uniform heat flux	Parallel isotherms	(k_d/k_c)	$1-\bar{\varepsilon}$	Ref.
34	Air 2.08	SiC 1550	20.0	12.8	266.2	745.1921	0.429	[12]
35	CO_2 1.26	SiC 1550	15.6	8.3	250.6	1230.1594	0.429	[12]
36	IC8 12.29	Silica 973.9	94.4	50.6	247.0	79.2727	0.428	[7]
37	IC8 12.29	Silica 973.9	94.0	50.7	247.0	79.2727	0.428	[7]
38	Glycerin 46.3	Glass 94	73.3	29.1	73.3	2.0289	0.428	[7]
39	Water 54.5	Silica 973.9	207.0	156.7	350.5	17.8689	0.426	[7]
40	Water 54.5	Silica 973.9	212.9	153.4	358.0	17.8689	0.426	[7]
41	Air 2.31	Silica 973.9	22.3	13.0	182.6	421.9353	0.426	[7]
42	IC8 12.29	Silica 973.9	70.9	50.4	248.4	79.2727	0.426	[7]
43	Air 2.31	Glass 94.0	18.5	8.1	27.9	40.7097	0.426	[7]
44	Helium 11.95	SiC 1550	61.5	54.4	357.5	129.7071	0.425	[8]
45	Hydrogen 14.85	SiC 1550	85.0	64.7	373.3	104.3771	0.425	[12]
46	Air 2.08	SiC 1550	22.6	12.7	267.7	745.1921	0.425	[12]
47	CO_2 1.26	SiC 1550	14.7	8.2	252.0	1230.1594	0.425	[12]
48	Air 2.31	Silica 973.9	22.6	13.0	182.6	421.9353	0.424	[7]
49	CO_2 1.2	SiO 700	16.3	7.1	125.0	583.3333	0.424	[7]
50	Air 2.41	SiO 700	23.8	12.8	139.5	290.4563	0.424	[7]
51	Air 2.41	SiO 700	23.4	12.8	139.5	290.4563	0.424	[7]
52	Air 2.41	SiO 700	25.2	12.8	139.5	290.4563	0.424	[7]
53	Glycerin 26.3	Silica 973.9	205.5	136.6	342.2	21.0289	0.424	[7]
54	Air 2.34	Steel 3850	44.6	15.7	608.0	1645.2996	0.423	[6]
55	EtOH 29.3	Silica 973.9	163.8	97.9	303.6	33.1980	0.423	[7]
56	EtOH 29.3	Glass 94.0	55.4	45.3	61.7	3.2030	0.423	[7]
57	Air 2.34	Lead 2950	36.0	15.3	478.3	1260.6841	0.420	[6]
58	Air 2.41	Glass 93.5	17.1	8.4	28.1	38.7967	0.420	[7]
59	Helium 11.95	Glass 93.5	34.2	25.9	44.3	7.8243	0.420	[7]
60	Helium 11.95	Glass 93.5	35.6	25.9	44.3	7.8243	0.420	[7]
61	EtOH 29.6	Glass 93.5	53.3	45.5	61.8	3.1588	0.420	[7]
62	EtOH 29.6	Glass 93.5	55.0	45.5	61.8	3.1588	0.420	[7]
63	Glycerol 45.4	Glass 93.5	71.4	58.1	73.8	2.0595	0.420	[7]
64	Water 51.6	Glass 93.5	71.6	62.3	78.1	1.8120	0.428	[7]
65	Water 51.6	Glass 93.5	71.4	62.3	78.1	1.8120	0.420	[7]
66	Water 51.1	Lead 3000	358.0	196.1	816.9	58.7084	0.420	[10]

Table 1 *Continued*

Case	Fluid phase	Solid phase	Conductivity, (kcal/m h K) × 100 Experiment	Uniform heat flux	Parallel isotherms	(k_d/k_c)	$1-\bar{\varepsilon}$	Ref.
67	IC8 12.3	Silica 973.9	70.7	50.4	248.4	79.2727	0.420	[7]
68	IC8 12.3	Silica 973.9	71.3	50.4	248.4	79.2727	0.419	[7]
69	EtOH 29.3	Silica 973.9	144.4	97.9	303.6	33.198	0.418	[7]
70	Air 2.34	Steel 3850	37.8	15.7	608.0	1645.2996	0.417	[6]
71	Air 2.48	Lead 2950	42.5	16.1	481.4	1189.5161	0.417	[13]
72	Air 2.25	Quartz 945	29.7	12.7	177.3	420.0	0.416	[11]
73	Air 2.34	Lead 2950	36.4	15.3	478.3	1260.6841	0.416	[6]
74	Air 2.308	Glass 94.0	17.1	8.1	27.9	40.7097	0.414	[7]
75	Water 54.5	Silica 973.9	230.8	153.4	358.0	17.8689	0.414	[7]
76	Air 2.34	Steel 3850	35.1	15.7	608.0	1645.2996	0.413	[6]
77	Hydrogen 14.85	SiC 1550	100.7	64.7	373.3	104.3771	0.410	[12]
78	Air 2.08	SiC 1550	22.4	12.7	267.7	745.1921	0.410	[12]
79	CO_2 1.26	SiC 1550	17.8	82.1	252.0	1230.1594	0.410	[12]
80	Air 2.86	Sand 187.5	20.7	11.3	49.9	65.6250	0.410	[14]
81	EtOH 29.3	Silica 973.9	154.9	97.9	303.6	33.1980	0.410	[7]
82	Water 54.5	Glass 94	73.1	64.3	80.2	1.7240	0.408	[7]
83	Air 2.31	Silica 973.9	24.6	13.0	182.6	421.9353	0.408	[7]
84	Air 2.34	Steel 3850	51.7	15.7	608.0	1645.2996	0.406	[6]
85	Air 2.14	Lead 3000	32.3	14.1	481.1	1401.8694	0.406	[10]
86	Air 2.48	Copper 32950	78.6	18.4	4700.0	13313.2539	0.403	[9]
87	Air 2.34	Steel 3850	36.8	15.7	608.0	1645.2996	0.402	[6]
88	Air 2.34	Steel 3850	47.5	15.7	608.0	1645.3	0.401	[6]
89	Air 2.14	Lead 3000	32.5	14.1	481.1	1401.9	0.401	[10]
90	Air 2.25	Lead 3030	37.0	14.8	487.9	1346.7	0.400	[11]
91	Hydrogen 16.6	Lead 3030	120.6	80.8	655.2	182.5	0.400	[11]
92	Water 54.5	Lead 3030	298.0	206.5	835.3	55.6	0.400	[11]
93	Glycerin 24.4	Lead 3030	176.0	110.1	704.9	124.2	0.400	[11]
94	Hydrogen 12.6	Glass 93.5	39.6	26.7	45.1	7.42	0.400	[13]
95	Air 2.48	Glass 93.5	15.5	8.6	28.3	37.7	0.400	[13]
96	Air 2.91	Steel 4500	53.2	19.4	714.8	1546.4	0.400	[14]
97	Air 2.91	Steel 4500	55.4	19.4	714.8	1546.4	0.400	[14]
98	Air 2.91	Steel 4500	58.5	19.4	714.8	1546.4	0.400	[14]
99	Air 2.91	Steel 4500	59.5	19.4	714.8	1546.4	0.400	[14]

Table 1 *Continued*

Case	Fluid phase	Solid phase	Conductivity, (kcal/m h K) × 100 Experiment	Uniform heat flux	Parallel isotherms	(k_f/k_s)	$1-\varepsilon$	Ref.
100	Air 2.91	Steel 4500	61.1	19.4	714.8	1546.4	0.400	[14]
101	Air 2.34	Cellite 92.0	23.4	8.2	27.5	39.3	0.400	[10]
102	Air 2.41	Coal 36.0	10.2	6.4	13.9	14.9	0.400	[10]
103	EtOH 15.7	Lead 3000	126.0	77.0	643.3	191.1	0.397	[7]
104	Air 2.34	Steel 3850	43.5	15.7	608.0	1645.3	0.394	[6]
105	Air 2.34	Steel 3850	51.7	15.7	608.0	1645.3	0.394	[6]
106	EtOH 29.3	Copper 33163	327.6	198.4	5197.1	1130.5	0.392	[7]
107	Air 2.34	Steel 3850	40.3	16.0	597.1	1645.3	0.391	[6]
108	Water 50.9	Lead 3000	327.0	193.5	824.8	58.9	0.391	[10]
109	Air 2.34	Steel 3850	44.6	15.6	614.4	1645.3	0.390	[6]
110	Air 2.85	Sand 187.6	26.3	11.1	50.4	65.6	0.390	[14]
111	Air 2.38	Quartz 950.1	41.8	13.2	181.7	398.7	0.390	[9]
112	EtOH 29.8	Copper 11500	318.0	163.7	2210.0	385.9	0.388	[7]
113	EtOH 29.8	Copper 11500	342.0	163.7	2210.0	385.9	0.388	[7]
114	Glycerin 45.4	Copper 11500	580.0	232.2	2370.0	253.3	0.388	[7]
115	Glycerin 45.4	Copper 11500	595.0	232.2	2370.0	253.3	0.388	[7]
116	Water 51.6	Copper 11500	550.0	257.8	2424.0	222.9	0.388	[7]
117	Water 51.6	Copper 11500	615.0	257.8	2424.0	222.9	0.388	[7]
118	Water 51.6	Copper 11500	630.0	257.8	2424.0	222.9	0.388	[7]
119	Water 54.5	Copper 33163	629.9	321.2	5950.6	608.5	0.387	[7]
120	Water 54.5	Copper 33163	597.1	321.2	5950.6	608.5	0.387	[7]
121	EtOH 29.33	Copper 33163	323.1	321.2	5950.6	1130.5	0.386	[7]
122	Glycerin 46.3	Copper 33163	607.6	321.2	5950.6	716.1	0.386	[7]
123	Glycerin 46.3	Copper 33163	549.5	187.5	5499.4	716.1	0.385	[7]
124	Water 54.5	Copper 33163	634.4	279.4	5818.1	608.5	0.384	[7]
125	Air 2.43	Steel 3030	45.0	15.7	497.1	1246.9	0.380	[15]
126	Methane 3.0	Steel 3300	55.8	19.1	548.9	1100.0	0.380	[15]
127	Propane 1.6	Steel 3300	35.0	10.9	516.5	2062.5	0.380	[15]
128	CO_2 1.35	Steel 3300	32.4	9.3	509.8	2444.4	0.380	[15]
129	Hydrogen 16.4	Steel 3300	188.0	80.4	708.4	201.2	0.380	[15]
130	Air 2.34	Steel 2850	45.7	15.1	468.7	1217.9	0.380	[6]
131	Oil 15.4	Lead 2410	101.0	72.0	541.9	156.5	0.380	[13]
132	Air 2.86	Sand 187.6	26.4	11.1	50.4	65.6	0.370	[14]

Table 1 *Continued*

Case	Fluid phase	Solid phase	Conductivity, (kcal/m h K) × 100 Experiment	Uniform heat flux	Parallel isotherms	(k_d/k_c)	$1-\bar{\varepsilon}$	Ref.
133	Air 2.25	Steel 2250	35.6	14.2	378.4	1000.0	0.365	[11]
134	Hydrogen 16.6	Steel 2250	110.0	75.5	520.0	135.5	0.365	[11]
135	Helium 11.95	Glass 93.5	31.1	25.6	44.8	7.8	0.350	[12]
136	Air 2.12	Glass 93.5	13.8	7.5	27.5	44.1	0.350	[12]
137	Air 20.8	Glass 59.1	13.8	6.61	19.4	28.3	0.349	[16]
138	Air 2.23	Lead 3030	34.2	14.5	492.6	1358.7	0.346	[17]
139	Hydrogen 14.9	SiC 1548.7	95.4	64.1	377.2	104.0	0.328	[16]
140	Air 2.08	SiC 1548.7	27.3	12.6	270.4	742.8	0.328	[16]
141	CO_2 1.27	SiC 1548.7	26.2	8.2	254.6	1223.5	0.328	[16]
142	Hydrogen 14.9	SiC 1548.7	61.7	64.1	377.2	104.0	0.325	[16]
143	Air 2.08	SiC 1548.7	27.0	12.6	270.4	742.9	0.325	[16]
144	CO_2 1.27	SiC 1548.7	25.2	8.2	254.6	1223.5	0.325	[16]
145	Air 2.38	Quartz 950.1	49.0	13.4	178.1	398.7	0.310	[9]
146	Hydrogen 14.9	SiC 1548.7	110.8	62.5	386.4	104.0	0.308	[16]
147	Air 2.08	SiC 1548.7	27.5	12.3	277.0	742.9	0.308	[16]
148	CO_2 1.27	SiC 1548.7	26.4	7.97	260.7	1223.5	0.308	[16]
149	Helium 12.0	SiC 1548.7	85.2	52.7	260.7	129.2	0.308	[16]
150	Air 2.25	Lead 3030	58.4	14.3	505.1	1346.7	0.310	[11]
151	Air 2.25	Quartz 945.0	70.0	12.2	183.5	420.0	0.276	[12]
152	Air 2.25	Quartz 945.0	76.0	12.2	183.5	420.0	0.241	[12]
153	Water 54.5	S.S. 1795.9	272.5	195.8	496.8	33.0	0.501	[7]
154	Glycerin 46.3	S.S. 1795.9	248.7	172.9	475.5	38.8	0.502	[7]
155	EtOH 29.3	S.S. 1795.9	172.7	120.7	422.3	61.2	0.505	[7]
156	Hydrogen 14.85	$(C_6H_5)_2NH$ 18.9	16.5	16.7	16.7	1.3	0.513	[12]
157	Air 2.08	$(C_6H_5)_2NH$ 18.9	6.9	5.1	7.5	9.1	0.513	[12]
158	Hydrogen 14.85	SiC 1550	46.0	68.3	322.1	104.4	0.518	[12]
159	CO_2 0.1578×10^{-7}	Basalt 90.7	0.1061	0.1280×10^{-6}	10.53	5.75×10^{9}	0.540	[8]
160	CO_2 0.1856×10^{-7}	Basalt 90.7	0.08183	0.1760×10^{-6}	9.0	4.89×10^{9}	0.600	[8]
161	CO_2 0.2373×10^{-7}	Basalt 90.7	0.05598	0.1933×10^{-6}	10.47	3.82×10^{9}	0.654	[8]
162	CO_2 0.2967×10^{-7}	Basalt 90.7	0.511	0.2747×10^{-6}	8.90	3.16×10^{9}	0.683	[8]
163	CO_2 0.4764×10^{-7}	Basalt 90.7	0.0414	0.181×10^{-6}	19.15	2.23×10^{9}	0.721	[8]
164	CO_2 0.1464×10^{-7}	Basalt 90.7	0.1404	0.652×10^{-6}	19.15	6.19×10^{9}	0.470	[12]
165	Air 2.08	SiC 1550	15.6	12.7	218.9	745.2	0.518	[12]

Table 1 *Continued*

Case	Fluid phase	Solid phase	Conductivity, (kcal/m h K) × 100 Experiment	Uniform heat flux	Parallel isotherms	(k_d/k_c)	$1-\bar{\varepsilon}$	Ref.
166	CO_2 1.26	SiC 1550	11.85	8.1	205.6	1230.2	0.518	[12]
167	Air 2.47	Iron 5628.9	39.9	13.2	584.0	2277.1	0.575	[9]
168	Oil 15.4	Copper 32000	130.0	80.6	3365.0	2077.9	0.580	[13]
169	Oil 15.4	Steel 3500	81.5	62.2	512.8	227.3	0.580	[10]
170	Oil 15.4	Glass 61.2	29.8	25.2	31.2	3.974	0.580	[10]
171	Oil 15.4	Lead 2410	60.0	58.7	381.7	156.5	0.580	[10]
172	CO_2 0.2013	Basalt 96.8	1.024	0.602	18.28	480.7	0.720	[8]

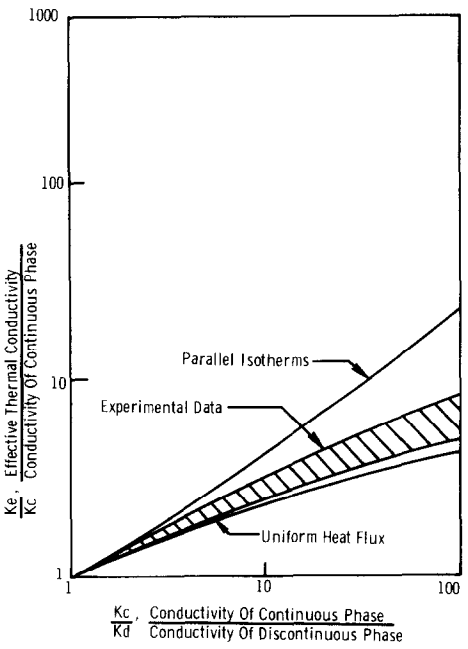

FIG. 6. Comparison of bounding conductivities with experimental data for a porosity of 0.43.

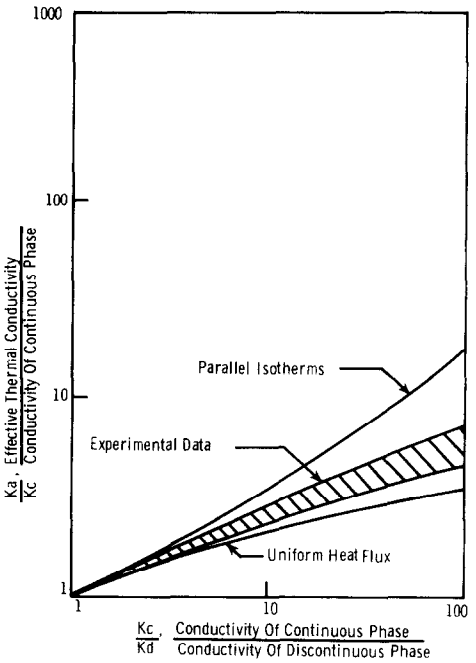

FIG. 7. Comparison of bounding conductivities with experimental data for a porosity of 0.58.

Thus the calculated equations are raised above the lower bounding curve. Similarly for parallel isotherm models an excessive amount of the higher conductivity material can be placed in parallel with itself and in series with the low conductivity phase. This distortion tends to result in a lower calculated conductivity than that of the upper bound.

The approach to be recommended here is to avoid all distortions of the granular system geometry. Recognizing that some error is introduced by the one dimensional heat transfer assumptions a correction factor is to be applied to one of the bounding equations. Such a correction factor must at the present time be obtained empirically. Selecting the upper bound equation an isothermal distortion factor, $\bar{F}_\infty$, may be introduced such that:

$$\bar{F}_\infty = \frac{\bar{k}}{k_{e\infty}}. \tag{19}$$

It is assumed that the isothermal distortion factor may be expressed as a polynomial function of the constituent conductivity ratio k_d/k_c and the solid fraction $\bar{\varepsilon}$. Using data from Table 1 values of $\bar{F}_\infty$ have been correlated using a least squares technique. The resulting correlation was found to be:

$$\ln \bar{F}_\infty = -0.1439 - 0.72359 \ln(k_d/k_c) + 0.020114[\ln(k_d/k_c)]^2 + 3.0260\bar{\varepsilon}. \tag{20}$$

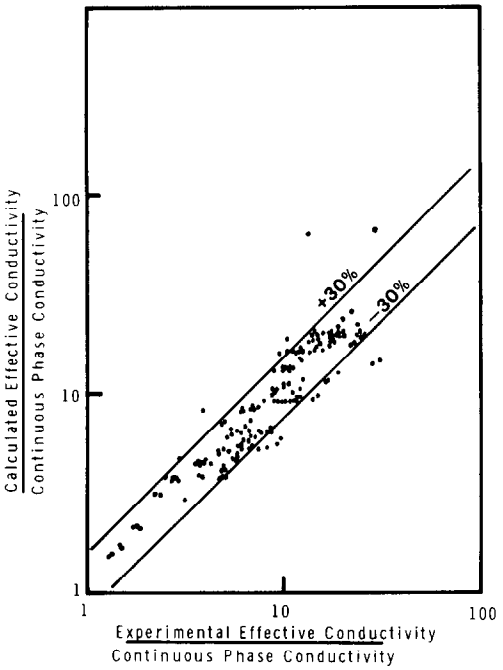

FIG. 8. Comparison of experimental and calculated results.

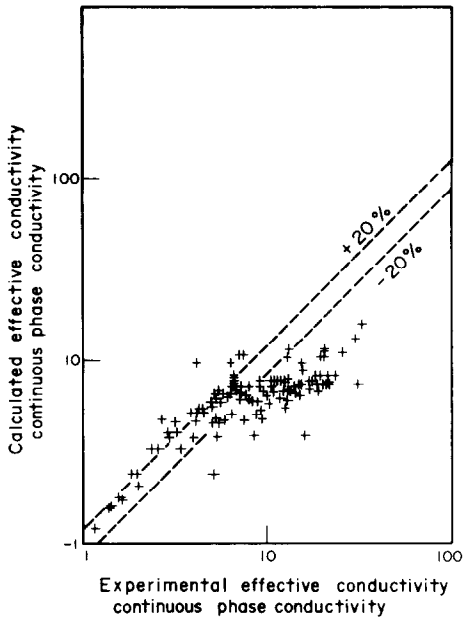

FIG. 10. Comparison of experimental results with calculated conductivity for the Meredith and Tobias equation.

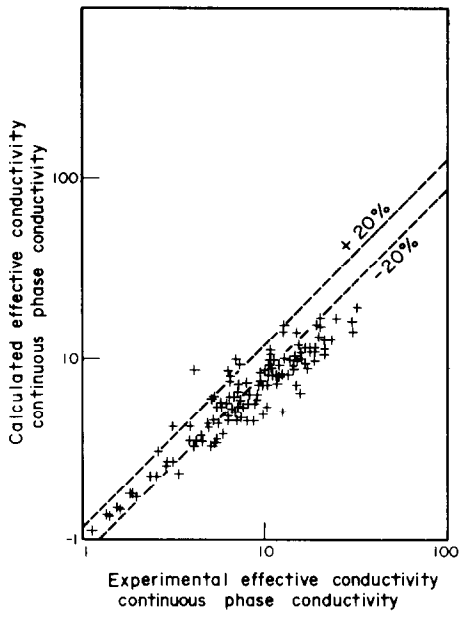

FIG. 9. Comparison of experimental results with calculated conductivity for the Schumann and Voss equation.

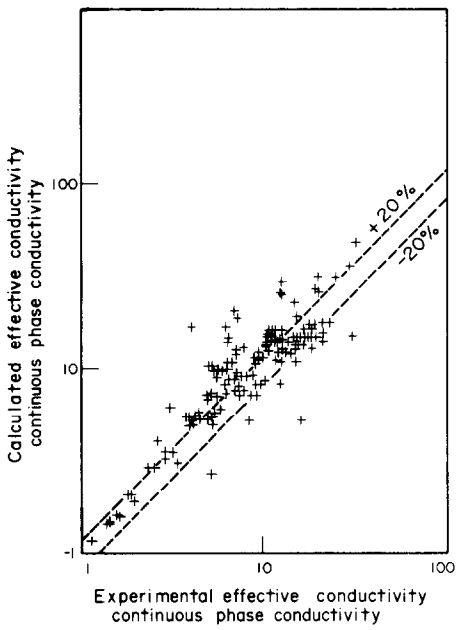

FIG. 11. Comparison of experimental results with calculated conductivity for the Bruggeman equation.

A comparison between predicted and calculated data from Table 1 is shown in Fig. 8. It should be noted that the correlation will fit virtually all of the data points within $\pm 30\%$. The average error is calculated to be 21%. This range of accuracy appears quite good in consideration of the variety of sources from which data was selected and the wide range of particle sizes and shapes included. Moreover it was necessary to assume certain constituent conductivities in that their exact composition was not always given by researchers.

For comparative purposes four well known correlations developed by Schumann and Voss [11], Meredith and Tobias [18], Bruggeman [19] and Lord Rayleigh [20] have been evaluated. Calculational results are illustrated in Figs. 9–12 respectively. The average error for these correlations is calculated to be 24.9, 31.6, 26.9 and 33.3% respectively. The new correlation is seen to reduce this average error significantly. The authors attribute this improvement to the assumed geometrical form.

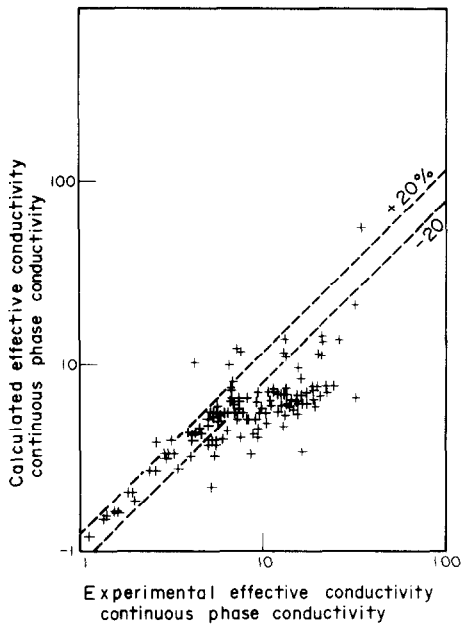

FIG. 12. Comparison of experimental results with calculated conductivity for the Lord Rayleigh equation.

In conclusion, two bounding equations to the effective thermal conductivity of granular materials have been developed. These equations indicate a limit to the usefulness of one dimensional models and hence to the Ohm's Law approach in evaluating such systems without empirical correlation. The model which has been proposed for evaluating the thermal conductivity of granular systems offers the unique advantage of being based on a geometrically realistic geometry. While distortion of the heat flux lines and isotherms can not yet be adequately handled by analytical development they are considered by means of an empirical curve fit. Thus both of the major factors affecting errors in simplified models have been avoided in this development.

REFERENCES

1. R. I. Vachon, A. G. Prakouras, R. A. Crane and M. S. Khader, Thermal conductivity of heterogeneous mixtures and lunar soils, Engineering Experiment Station, Auburn University, Contract No. NAS8-26579 (October 1973).
2. G. T. Tsao, Thermal conductivity of two-phase materials, *Ind. Engng Chem.* **53**(5), 395 (1961).
3. S. Debbas and H. Rumpf, On the randomness of beds packed with spheres or irregular shaped particles, *Chem. Engng Sci.* **21**, 583 (1966).
4. D. P. Haughey and G. S. G. Beveridge, Local voltage variation in a randomly packed bed of equal sized spheres, *J. Engng Sci.* **21**, 905 (1966).
5. K. Stange, The mixing of random systems as a basis for estimating mixing data, *Chem.-Ingr.-Tech.* **6**, 331 (1954).
6. A Waddams, The flow of heat through granular materials, *J. Soc. Chem. Ind.* **63**, 337 (1944).
7. F. W. Preston, Mechanism of heat transfer in unconsolidated porous media at low flow rates, Ph.D. Dissertation, Penn. State University (1957).
8. J. A. Fountain and E. A. West, Thermal conductivity of particulate basalt as a function of density in simulated lunar and martian environments, *J. Geophys. Res.* **75**(20), 4063 (1970).
9. R. L. Goring and S. W. Churchill, Thermal conductivity of heterogeneous materials, *Chem. Engng Progr.* **57**(7), 53 (1961).
10. R. Krupiczka, Analysis of thermal conductivity in granular materials, *Chemia Stosow.* **2B**, 183 (1966).
11. T. E. W. Shumann and V. Voss, Heat flow through granulated material, *Fuel Sci. Practice* **13**, 249 (1934).
12. R. H. Wilhelm, W. C. Johnson, R. Wynkoop and O. H. Collier, Reaction rate, heat transfer and temperature distribution in fixed-bed catalytic converters, *Chem. Engng Prog.* **44**(2), 105 (1948).
13. H. Vershoor and G. C. A. Schuit, Heat transfer to fluids flowing through a bed of granular solids, *Appl. Scient. Res.* **42**, 97 (1950).
14. S. Yagi and D. Kunii, Studies on effective thermal conductivities in packed beds, *A.I.Ch.E. Jl* **3**, 373 (1957).
15. G. Kling, The heat conduction of spherical aggregates in still gases, *ForschHft. Ver. Dt. Ing.* **9**, 28 (1938).
16. W. G. Kannuluik and L. H. Martin, Conduction of heat in powders, *Proc. R. Soc. Lond.* **A141**, 144 (1933).
17. D. A. DeVries, *Physics of Plant Environment*, 2nd edn, p. 210. North Holland, Amsterdam (1966).
18. R. E. Meredith and C. W. Tobias, Resistance to potential flow through a cubical array of spheres, *J. Appl. Phys.* **31**, 1270 (1960).
19. D. A. G. Bruggeman, Dielectric constant and conductivity of mixtures of isotropic materials, *Ann. Phys.* **24**, 636 (1935).
20. Lord Rayleigh, On the influence of obstacles arranged in rectangular order upon the properties of a medium, *Phil. Mag. J. Sci.* **34**, 481 (1892).

ESTIMATION DES LIAISONS POUR LE CALCUL DE LA CONDUCTIVITE THERMIQUE EFFECTIVE DES MATERIAUX GRANULEUX

Résumé—Pour décrire la conductivité thermique effective de systèmes de grains agglomérés au hasard, on développe deux modèles basés sur la méthode de la loi d'Ohm monodimensionnelle. Ces modèles représentent les liaisons supérieures et inférieures pour tous les mélanges stochastiques normalement distribués. On obtient un facteur empirique pour tenir compte des effets thermiques tridimensionnels. Des comparaisons avec les résultats expérimentaux indiquent que la corrélation modifiée est généralement correcte à $\pm 20\%$ pour une large gamme de matériaux constitutifs.

BESTIMMUNG DER GRENZWERTE DER EFFEKTIVEN WARMELEITFAHIGKEIT GRANULIERTER MATERIALIEN

Zusammenfassung—Zur Beschreibung der effektiven Wärmeleitfähigkeit von Granulatsystemen willkürlicher Packung werden zwei auf dem eindimensionalen Ohmschen Gesetz basierende Modelle entwickelt. Diese Modelle geben die obere und untere Grenze der effektiven Wärmeleitfähigkeit für eine normal verteilte stochastische Mischung wieder. Mit Hilfe eines empirischen Faktors werden dreidimensionale Wärmeleiteffekte erfaßt. Ein Vergleich mit Meßwerten zeigt, daß die modifizierte Beziehung für eine Vielzahl von Materialien uauf $\pm 20\%$ genau stimmt.

РАСЧЕТ ГРАНИЦ ЭФФЕКТИВНОЙ УДЕЛЬНОЙ ТЕПЛОПРОВОДНОСТИ ЗЕРНИСТЫХ МАТЕРИАЛОВ

Аннотация — Разработаны две модели для описания эффективной удельной теплопроводности дисперсных систем с беспорядочной укладкой частиц на основании одномерного метода закона Ома. Показано, как эти модели определяют верхнюю и нижнюю границы эффективной удельной теплопроводности всех стохастических смесей с нормальным распределением. Получен эмпирический коэффициент для учета трехмерных тепловых эффектов. Сравнение с экспериментальными данными показывает, что модифицированная корреляция имеет точность около $\pm 20\%$ для широкого диапазона компонентов смеси.